DOI: 10.61782/fa.2023.1217

forum acusticum 2023

GAUSSIAN ORTHOGONAL ENSEMBLE MODELLING OF BUILT-UP SYSTEMS WITH DOMAIN COUPLINGS ON DIFFUSE COMPONENTS

Cédric Van hoorickx[1,2*] **Edwin P.B. Reynders**[1]
[1] KU Leuven, Department of Civil Engineering, Structural Mechanics Section, Belgium
[2] Eindhoven University of Technology, Department of the Built Environment, Building Acoustics group, The Netherlands

ABSTRACT

If the wavelength is small compared to the characteristic size (e.g., mean free path) of a system component, it can be modelled as diffuse. Recently, a method of analysis was developed to compute the detailed response field of built-up systems containing both diffuse and deterministic vibro-acoustic components. In this method, diffuse field realizations are generated in a Monte Carlo framework, from which the joint probability density function of the response can be obtained. The approach is computationally efficient because the natural frequencies and mode shapes of the diffuse components are directly drawn from universal probability distributions: the local eigenvalue spacings conform to the Gaussian Orthogonal Ensemble and the mode shapes are zero-mean Gaussian random fields. So far, only discrete couplings between system components have been investigated, whereas in practical applications, components may be coupled over a domain (e.g., the surface of a plate when coupled with an acoustic volume). In this contribution, domain couplings are established by generating realizations of coupling terms appearing in the coupled equilibrium equations. The probability density functions of these coupling terms are derived analytically to enable computationally efficient realizations. The method is applied to analyze the sound field in an aircraft cabin.

Keywords: *vibro-acoustics, diffuse sound field, domain couplings, uncertainty quantification*

Corresponding author: c.m.l.van.hoorickx@tue.nl.

1. INTRODUCTION

Diffuse or reverberant field models are widely employed for vibro-acoustic analysis at high frequencies because of their computational efficiency and because they inherently account for uncertainty related to small spatial variations in geometry, material properties, or boundary conditions, having a wave scattering effect. Statistical Energy Analysis (SEA) is frequently employed for analyzing built-up systems with diffuse components. When a system is analyzed with SEA, the total ensemble averaged vibrational energy in each of the diffuse components is obtained. Vibro-acoustic systems with domain couplings have been previously analyzed using the hybrid deterministic-SEA framework [1]. However, the capabilities of SEA-related approaches to analyze built-up systems with diffuse components have some limitations, such as: the displacement fields are not modelled but only the related energies, the joint response probability function is not available, and the computational efficiency decreases when there is additional parametric uncertainty.

A new method of analysis that overcomes those limitations was recently developed [2, 3]. Instead of modeling diffuse fields in the conventional way, a Monte Carlo (MC) technique is employed. Samples of the natural frequencies and mode shapes of the decoupled diffuse subsystems are directly obtained with a Gaussian random number generator, as they relate to a Gaussian Orthogonal Ensemble (GOE) matrix and a Gaussian random field, respectively. This method has been termed the GOE-MC method. However, the approach as presented in [2, 3] becomes computationally costly for domain couplings between components as modeshape realizations are needed over the entire area junction. Generation of diffuse modeshapes can be efficiently performed for acoustic cavities

by making use of prolate spheroidal wave functions, as demonstrated in [4], but still requires their storage and processing.

In the present work, the statistics of the coupling terms is derived such that realizations of these terms can be made instead of the modeshapes. This is computationally efficient as (i) no modeshape realizations over the entire area junction need to be computed and (ii) the integration of the modeshapes over this area does not need to be repeated for every realization. In this paper, fluid-structure domain coupling is discussed first. The GOE-MC methodology is used as framework for the presented approach and is described next. Then, the statistics of the coupling terms are discussed. Finally, an example of sound radiation by an aircraft fuselage to the cabin illustrates the presented approach.

2. FLUID-STRUCTURE DOMAIN COUPLING

Consider a built-up system consisting of a mixture of acoustic and structural system components. The response in the system components is computed here using the assumed-modes method. In the assumed-modes method, the pressure fields of the acoustic volumes p_a and the vibration field of the structural surfaces $\mathbf{u}$ at angular frequency ω are approximated into a finite set of modeshapes $\phi_{\mathrm{p}i}(\mathbf{x})$ and $\boldsymbol{\phi}_{\mathrm{u}i}(\mathbf{x})$:

$$\hat{p}(\mathbf{x},\omega) = \sum_i \phi_{\mathrm{p}i}(\mathbf{x}) q_{\mathrm{p}i}(\omega), \tag{1}$$

$$\hat{\mathbf{u}}(\mathbf{x},\omega) = \sum_i \boldsymbol{\phi}_{\mathrm{u}i}(\mathbf{x}) q_{\mathrm{u}i}(\omega). \tag{2}$$

The generalized pressure $q_{\mathrm{p}i}(\omega)$ of the acoustic volume Ω with prescribed generalized displacements $q_{\mathrm{u}k}(\omega)$ acting on its boundaries $\partial\Omega_\mathrm{i}$ can be obtained from:

$$\left(\omega_{\mathrm{p}i}^2 - \omega^2\right) q_{\mathrm{p}i} + \sum_k K_{\mathrm{pu},ik} q_{\mathrm{u}k} = \hat{f}_{\mathrm{p}i} \tag{3}$$

$$\text{with } K_{\mathrm{pu},ik} = -\rho\omega^2 \int_{\partial\Omega_\mathrm{i}} \phi_{\mathrm{p}i}\phi_{\mathrm{w}k}\mathrm{d}\mathbf{x}, \tag{4}$$

where $\omega_{\mathrm{p}i}^2$ are the eigenvalues of the pressure field in the acoustic component, $\hat{f}_{\mathrm{p}i}$ the modal pressure loading, and $\phi_{\mathrm{w}i} = \boldsymbol{\phi}_{\mathrm{u}i} \cdot \mathbf{n}$ with $\mathbf{n}$ the normal to the fluid-structure interface. Similarly, the generalized displacements of the structural components coupled with acoustic subsystems follow from:

$$\left(\omega_{\mathrm{u}i}^2 - \omega^2\right) q_{\mathrm{u}i} + \sum_k K_{\mathrm{up},ik} q_{\mathrm{p}k} = \hat{f}_{\mathrm{u}i} \tag{5}$$

$$\text{with } K_{\mathrm{up},ik} = \int_{\partial\Omega_\mathrm{i}} \phi_{\mathrm{w}i}\phi_{\mathrm{p}k}\mathrm{d}\mathbf{x}, \tag{6}$$

where $\omega_{\mathrm{u}i}^2$ are the eigenvalues of the displacement in the structural system component. The coupled fluid-structure analysis consists of solving Eq. (3) and (5) simultaneously for the different system components.

3. THE GOE-MC METHODOLOGY

The GOE-MC approach is now used to obtain the response of built-up systems containing components that are either entirely deterministic or entirely diffuse. It uses Monte Carlo (MC) simulations, in which each sample represents the realization of a diffuse field. The response for every realization is computed based on the fact that the statistics of the local eigenvalue spacings are those of the GOE, while the modeshapes are Gaussian random fields.

The procedure for generating the natural frequencies is summarized below, and can be found in detail in [3]. Note that to perform the analysis across the entire frequency range of interest, the range of computed natural frequencies is larger than the frequency range of analysis as some out-of-band modes should also be considered.

The first step is to estimate the number of expected eigenfrequencies $N_\mathrm{int} = N(\omega_\mathrm{u})$ up to the upper frequency ω_u. The mode count can be obtained from the modal density:

$$N(\omega) = \int_0^\omega n(\omega')\mathrm{d}\omega'. \tag{7}$$

The second step is to make realizations of a Gaussian Orthogonal Ensemble (GOE) matrix with a random number generator. The GOE matrix is a real symmetric matrix with independent, centered Gaussian random variables as entries: the diagonal entries have variance $2\sigma_\mathrm{G}^2$ and the off-diagonal entries have variance σ_G^2, where the parameter σ_G serves to specify an eigenvalue scale. The size of the GOE matrix should be such that the number of rows or columns n_G is considerably larger than the number of eigenfrequencies N_int. Subsequently, its eigenvalues need to be computed. Alternatively, previously computed and tabulated GOE eigenvalues can be re-used as the eigenvalues do not depend on any physical properties.

The third step is to determine the range of GOE eigenvalues $[-\lambda_{\mathrm{Gl}}, \lambda_{\mathrm{Gl}}]$ such that the cumulative count function $N_{\mathrm{G}}(\lambda_{\mathrm{Gl}})$ equals N_{int}. Based on an expression for the density of the GOE eigenvalues for $n_{\mathrm{G}} \to \infty$ as proven by Wigner [5], the cumulative count function is obtained as:

$$N_{\mathrm{G}}(\lambda_{\mathrm{G}}) = \frac{n_{\mathrm{G}}}{\pi r_{\mathrm{G}}^2}\left(\lambda_{\mathrm{Gl}}\sqrt{r_{\mathrm{G}}^2-\lambda_{\mathrm{Gl}}^2}+\lambda_{\mathrm{G}}\sqrt{r_{\mathrm{G}}^2-\lambda_{\mathrm{G}}^2}\right) + \frac{n_{\mathrm{G}}}{\pi}\left(\arcsin\frac{\lambda_{\mathrm{Gl}}}{r_{\mathrm{G}}}+\arcsin\frac{\lambda_{\mathrm{G}}}{r_{\mathrm{G}}}\right) \tag{8}$$

with $r_{\mathrm{G}} = 2\sigma_{\mathrm{G}}\sqrt{n_{\mathrm{G}}}$.

Finally, the GOE eigenvalue realizations are transformed into the physical subsystem's eigenvalue realizations $\lambda := \omega^2$

$$\lambda = N^{-1}\left(N_{\mathrm{G}}(\lambda_{\mathrm{G}})\right) \tag{9}$$

4. COUPLING TERM REALIZATIONS

In contrast to [3], where diffuse modeshapes were generated, realizations of the coupling terms can be generated as will be demonstrated. The advantage is that the modeshapes do not need to be generated and the integration over the coupling area does not need to be performed for each realization. This makes this approach computationally efficient for surface couplings between acoustic and structural components.

The coupling terms $K_{\mathrm{pu},ik}$ and $K_{\mathrm{up},ik}$ in Eqs. (3) and (5) depend on the modeshapes of the system components, which in high-frequency regime are zero-mean, Gaussian random fields. The coupling terms are related ($K_{\mathrm{pu},ik} = -\rho\omega^2 K_{\mathrm{up},ki}$), so the computation of one of the coupling terms is sufficient to obtain both. As the modeshapes are zero-mean Gaussian random fields, the coupling terms are also Gaussian with following statistics:

$$\mathrm{E}\left[K_{\mathrm{up},ik}\right] = 0, \tag{10}$$

$$\mathrm{E}\left[K_{\mathrm{up},ik}^2\right] = \int_{\partial\Omega_{\mathrm{i}}}\int_{\partial\Omega_{\mathrm{i}}} C_{\mathrm{wi}}(\mathbf{x},\mathbf{x}')C_{\mathrm{pk}}(\mathbf{x},\mathbf{x}')\mathrm{d}\mathbf{x}\mathrm{d}\mathbf{x}'. \tag{11}$$

If the spatial covariance functions $C_{kj}(\mathbf{x},\mathbf{x}')$ of the modeshapes of the diffuse component(s) are known, these integrals can be computed directly. The main advantage here is that the integration over the surface only needs to be performed once, and therefore not for every mode shape realization.

For diffusely reflecting boundaries, the mode shapes ϕ_{kj} of system component k are statistically homogeneous, i.e., the statistics of the mode shape components are independent of their position. The corresponding random wave field is a diffuse field. The covariance function of a diffuse field can be obtained from the free-space Green's function $G_\infty(\mathbf{x},\mathbf{x}';\omega)$, i.e., the frequency response function of the corresponding unbounded system [6]:

$$C_{kj}(\mathbf{x},\mathbf{x}') = \mathrm{E}\left[\phi_{kj}(\mathbf{x})\phi_{kj}(\mathbf{x}')\right] \tag{12}$$

$$= \frac{-2\omega_{kj}}{\pi n_k(\omega_{kj})}\mathrm{Im}\left\{G_\infty(\mathbf{x},\mathbf{x}';\omega_{kj})\right\}. \tag{13}$$

In homogeneous and isotropic media, the evaluation of Eq. (13) results in the following expressions:

$$C_{kj}(\mathbf{x},\mathbf{x}') = \begin{cases} A_k\cos(k_{kj}||\mathbf{x}-\mathbf{x}'||) & \text{for 1D systems} \\ A_k\mathrm{J}_0(k_{kj}||\mathbf{x}-\mathbf{x}'||) & \text{for 2D systems} \\ A_k\mathrm{j}_0(k_{kj}||\mathbf{x}-\mathbf{x}'||) & \text{for 3D systems} \end{cases} \tag{14}$$

which corresponds to expressions found in e.g. [7]. In these expressions, $\mathrm{J}_0(x)$ denotes the Bessel function of the first kind and order zero, $\mathrm{j}_0(x) = \sin(x)/x$ is the spherical Bessel function of the first kind and order zero, $k_{kj} := \frac{2\pi}{\lambda_{kj}}$ denotes the wavenumber corresponding to the wavelength λ_{kj} of mode j for system component k, and A_k is a factor that is independent of position, which can be determined from the mode shape normalization condition. For acoustic subsystems, the normalization to unit modal mass yields $A_k = c^2/V_k$ with c the wave speed and V_k the total volume of the subsystem. The correlation function (14) depends only on the distance between the considered mode shape components, the wavelength, and the normalization condition. When the distance between $\mathbf{x}$ and $\mathbf{x}'$ is large compared to the wavelength λ_{kj}, it follows from the above expressions that in two-dimensional and three-dimensional subsystems, the mode shapes evaluated at these distinct points are approximately uncorrelated.

5. EXAMPLE

5.1 Problem description and finite element model

We illustrate this approach by computing the interior noise in a section of an aircraft cabin, as presented in [8]. It consists of a part of the aircraft fuselage that is excited at its wing connections, resulting in sound radiation radiated inside the cabin. The fuselage has a radius of $R = 1.866\,\mathrm{m}$ and is built up from $t = 1.125\,\mathrm{mm}$ thick flexible panels which are riveted to a stiffening frame. The geometry of this stiffening frame matches the airframe layout of a DC-8 fuselage as documented in [9].

The circumferential frames are located every $0.508\,\mathrm{m}$ in the axial direction and consist of Z profiles with a thickness of $1.125\,\mathrm{mm}$, a height of $63.5\,\mathrm{mm}$, and a flange width of $20.3\,\mathrm{mm}$ at both sides. Attached to these Z profiles are L profiles with a thickness of $1.125\,\mathrm{mm}$ and a length of $91.6\,\mathrm{mm}$ every $183.2\,\mathrm{mm}$. They have a height of $63.5\,\mathrm{mm}$, a width of $20.3\,\mathrm{mm}$ and they protrude $25.4\,\mathrm{mm}$ above the Z profiles. Hat-shaped longitudinal stringers are located on top of the Z profiles and have a thickness of $1.125\,\mathrm{mm}$. They have a height of $25.4\,\mathrm{mm}$, while the hat and the two brims all have a width of $16.9\,\mathrm{mm}$.

The aircraft fuselage is modelled using finite elements in Ansys, as illustrated in Fig. 1. Only a section of length $L_\mathrm{z} = 1.524\,\mathrm{m}$ is modelled. A zero displacement is therefore imposed along the axial direction ($z = 0$ and $z = L_\mathrm{z}$) to emulate the fact that the section is part of a much larger structure. Furthermore, since the section is considered to be symmetric, only a quarter section is modelled. Symmetry boundary conditions are therefore applied along the longitudinal boundary conditions ($x = 0$ and $y = 0$). This means that the displacements in the direction perpendicular to the plane of symmetry are imposed to be zero, as are the rotations around the other two axes. The structural components are produced out of an aluminium alloy with a Young's modulus of $70\,\mathrm{GPa}$, a Poisson's ratio of 0.3, a mass density of $\rho_\mathrm{s} = 2790\,\mathrm{kg/m^3}$, and a damping ratio of 0.01.

The fuselage is coupled to the acoustic cavity inside the aircraft. Along all faces of this acoustic cavity, zero normal velocity conditions are imposed. The cavity is filled with air, which has a mass density $\rho_\mathrm{a} = 1.1225\,\mathrm{kg/m^3}$ and a speed of sound $c = 340\,\mathrm{m/s}$. The reverberation time in the cavity is assumed to equal $1.0\,\mathrm{s}$ at all frequencies. In order to excite the system, two beams with a very high bending and torsional stiffness are attached to the fuselage (Fig. 1) and a unit structural point force is exerted at the endpoint where the beams meet, i.e. at $(2.7990\,\mathrm{m}, 0.9593\,\mathrm{m})$. This corresponds to a simplified representation of the shear forces and bending moments introduced by the wings on the fuselage connections.

The mode count of the fuselage is displayed in Fig. 2. Below $200\,\mathrm{Hz}$, there are only 8 modes, some of which are displayed in Fig. 3. The modal behaviour of the fuselage is therefore expected to play an important role in this frequency range. The first modes displayed in Fig. 3 are global flexural modes. At higher frequencies, local modes start to exist (e.g., mode 10), where the main deflection is situated between the stiffeners, i.e., at the flexible plate parts. From about $200\,\mathrm{Hz}$, local modes exist, and the mode count increases rapidly, up to 175 at $500\,\mathrm{Hz}$. This means that the modal behaviour of the fuselage becomes less important.

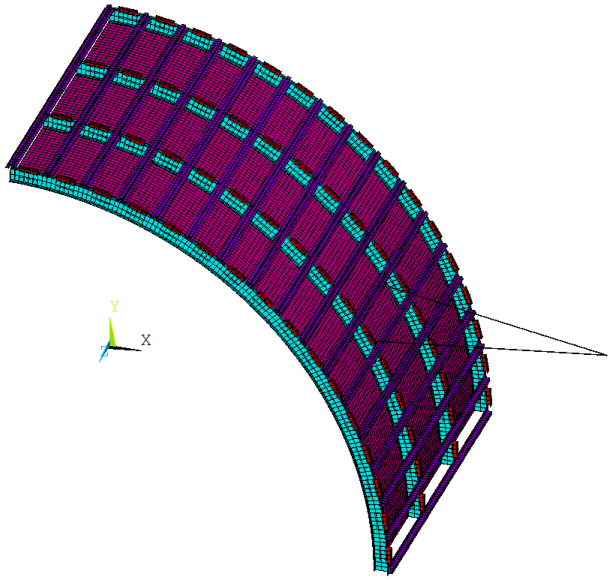

Figure 1. Finite element model of the DC-8 aircraft fuselage.

5.2 Numerical models

In an aircraft cabin, many wave scattering elements (e.g., seats, suitcases, passengers, etc.) are present. In this example, the cabin is assumed to have a random acoustic mass distribution in the sense that a total of 20 point air pockets (or acoustic point masses) are distributed at random locations within each room. The air pockets are highly idealized models for small wave scatterers in the room, in the same way as point masses would be highly idealized models for small wave scatterers on a plate. Each air pocket has $2\,\%$ of the total acoustic mass V/c^2 of the room. The probability distribution of the location of each air pocket is uniform throughout the entire room, and the locations of the air pockets are statistically independent.

The total number of air pockets and their individual acoustic mass are chosen arbitrarily; the important point is that, from a certain frequency onwards, the randomness introduced by the wave scatterers reaches a state of maximum information entropy, which conforms to a diffuse field. With a larger number of masses and/or a higher in-

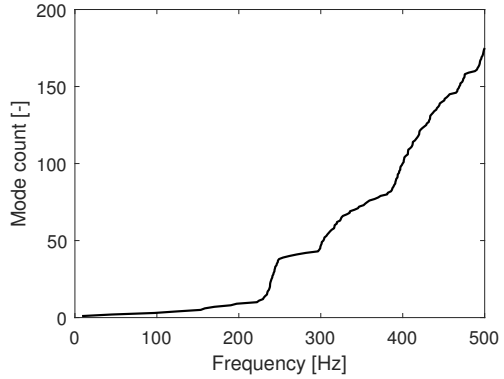

Figure 2. Mode count of the aircraft fuselage.

dividual acoustic mass, this state would occur already at a lower frequency than in the present case.

Two stochastic models for the cabin are constructed, and the mean and variance of the predicted quantities such as the spatially averaged (over the entire room volume) sound pressure level, are subsequently compared.

The first room model is a detailed model, in which both the point air pockets and the modal behaviour of the cabin are modelled in detail. In this method, random wave scatterers are modelled explicitly. This requires a detailed model of the system components, which can be obtained with e.g. the finite element method [10–12] for components of arbitrary complexity, or the Lagrange-Rayleigh-Ritz method [13, 14] for simple system components. As the wave scatterers are modelled explicitly, this yields the exact response, which is therefore considered to be the reference solution with which the presented approach can be compared. Because of its computational efficiency, the Lagrange-Rayleigh-Ritz method is often employed in conjunction with Monte Carlo (MC) simulation for generating reference solutions for systems with small random wave scatterers [2, 15–17]. It is therefore termed here the detailed MC method.

The second room model is a diffuse field model that is constructed as detailed in this paper and is termed the GOE-MC approach. In this model, the random wave scattering caused by placing the point air pockets at random locations within the room, is supposed to result in a diffuse sound field. The structural fuselage is then modelled deterministically with the finite element model from the previous section, while the cabin is modelled as diffuse. The two parameters needed for the numerical computations are the modal density or mode count and the spatial mode correlation function of the cavity. For the latter, the expression in Eq. (14) for 3D systems is used. For the mode count, the following expression is used [18]:

$$N(f) = \frac{4\pi V}{3}\left(\frac{f}{c}\right)^3 + \frac{\pi S}{4}\left(\frac{f}{c}\right)^2 + \frac{P}{8}\frac{f}{c}, \qquad (15)$$

where, in this case, $V = \pi R^2 L_z/4$, $S = \pi R/2 + \pi R^2/2 + 2RL_z$ and $P = \pi R + 4R + 3L_z$.

Note that in a diffuse field model, the physical mechanisms behind the wave scattering are not important. This second model would therefore provide exactly the same results when the random wave scattering would be caused by other types of wave scatterers than point air pockets, such as small hard objects of any shape, or irregular room boundaries. For this reason, the properties of the scattering elements (in the present case, the point air pockets) are not employed in the diffuse field model.

5.3 Sound radiation into the aircraft cabin

Using both models detailed in the previous section, the coupled system of Eqs. (3)-(5) is solved and the total energy E of the cabin is computed from:

$$E = \frac{1}{4\rho\omega^2}\sum_i \left(\omega^2 + \omega_{\mathrm{p}i}^2\right)|q_{\mathrm{p}i}|^2. \qquad (16)$$

Figure 4a-b display the ensemble average and the variance of the total energy in the room computed with the detailed MC approach and the presented GOE-MC approach. For the mean energy, a good agreement between both is obtained. The modal peaks corresponding to the modes of the fuselage (Fig. 3) are clearly distinguishable for both models. Some deviations at low frequencies are present as a result of the modal behaviour of the acoustic cavity, whose modal density is still very low and influence the interaction between the fuselage and the cavity. The variance of the total energy is well predicted at higher frequencies, but is overestimated by the diffuse field model at the lowest frequencies. This is because in that low-frequency range, the sensitivity of the local harmonic sound field to the presence of the small random wave scatterers (point air pockets) is relatively low, and a diffuse field model will overestimate the uncertainty caused by these random wave scatterers. However, once this sensitivity is sufficiently large, the diffuse field model is adequate.

For each Monte Carlo sample (both in the detailed MC and GOE-MC approach), the sound pressure level is

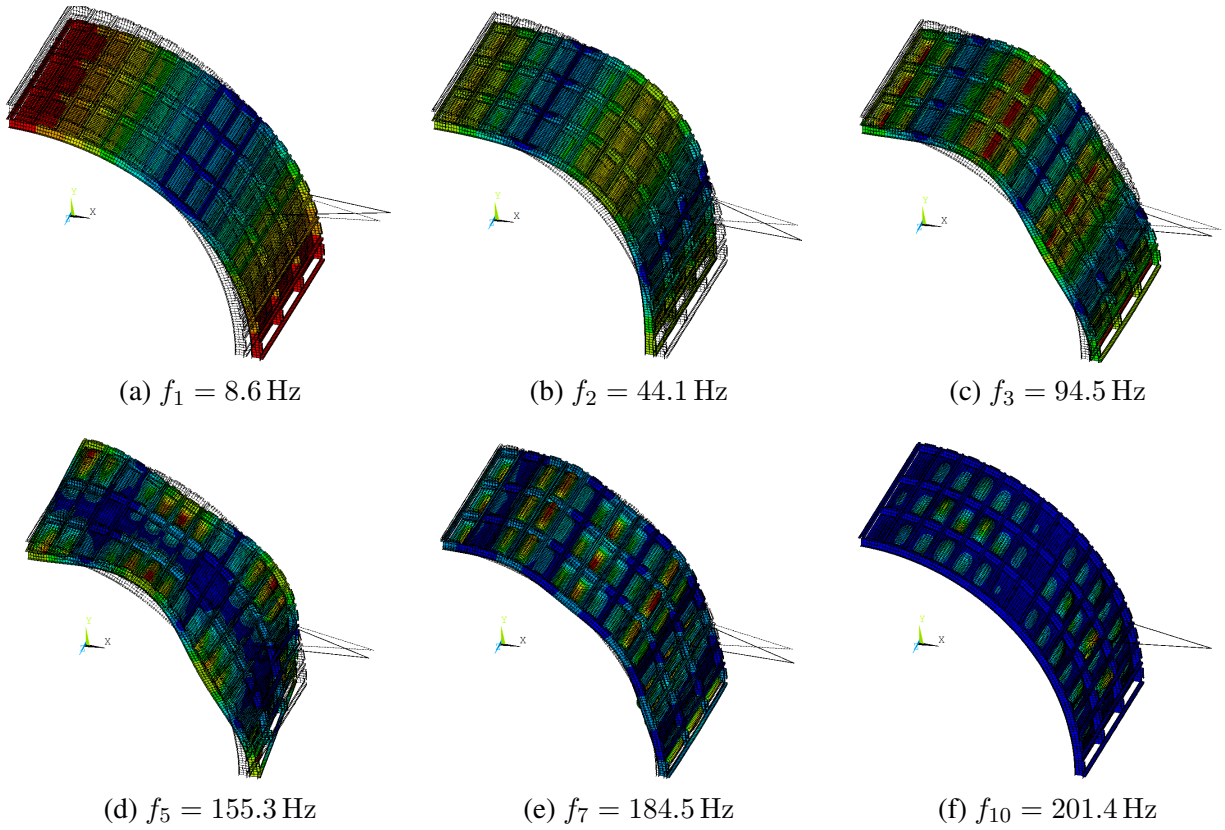

(a) $f_1 = 8.6\,\mathrm{Hz}$ (b) $f_2 = 44.1\,\mathrm{Hz}$ (c) $f_3 = 94.5\,\mathrm{Hz}$

(d) $f_5 = 155.3\,\mathrm{Hz}$ (e) $f_7 = 184.5\,\mathrm{Hz}$ (f) $f_{10} = 201.4\,\mathrm{Hz}$

Figure 3. Illustration of some modes of the aircraft fuselage.

obtained from the relation between the total energy and the time- and space-averaged squared sound pressure p_{av}^2 in diffuse fields [19]:

$$E = \frac{p_{\mathrm{av}}^2 V}{\rho c^2}. \tag{17}$$

The sound pressure level is then obtained from the time- and space-averaged squared sound pressure p_{av}^2:

$$L_{\mathrm{p}} = 10 \log \frac{p_{\mathrm{av}}^2}{p_0^2}, \tag{18}$$

where $p_0 = 20 \mu Pa$.

Figure 4c-d display the ensemble average and the variance of the sound pressure level computed in this way with both methods. The same conclusions can be made regarding the variance of the sound pressure level. However, the ensemble average of the sound pressure level is now underestimated by the GOE-MC approach. The reason is related to the fact that the mean of a logarithm is not equal to the logarithm of the mean. Instead, the mean of a logarithm depends both on the mean and variance of the argument. As the variance of the energy is overestimated at low frequencies, the mean of the logarithm of the energy, or the sound pressure level, is underestimated.

One advantage of the presented GOE-MC approach is that the probability density function can be estimated. This is illustrated in Figure 5 for the total energy in the cavity at six frequencies going from 150 Hz to 400 Hz in increments of 50 Hz. Although there is a small shift in the curves related to the predicted mean energy that is slightly under- or overestimated, the shape of the probability density function is usually well predicted, with a distinctive right tail.

6. CONCLUSIONS

In this contribution, the statistics of coupling terms have been derived for vibro-acoustic built-up systems with domain couplings between diffuse and deterministic compo-

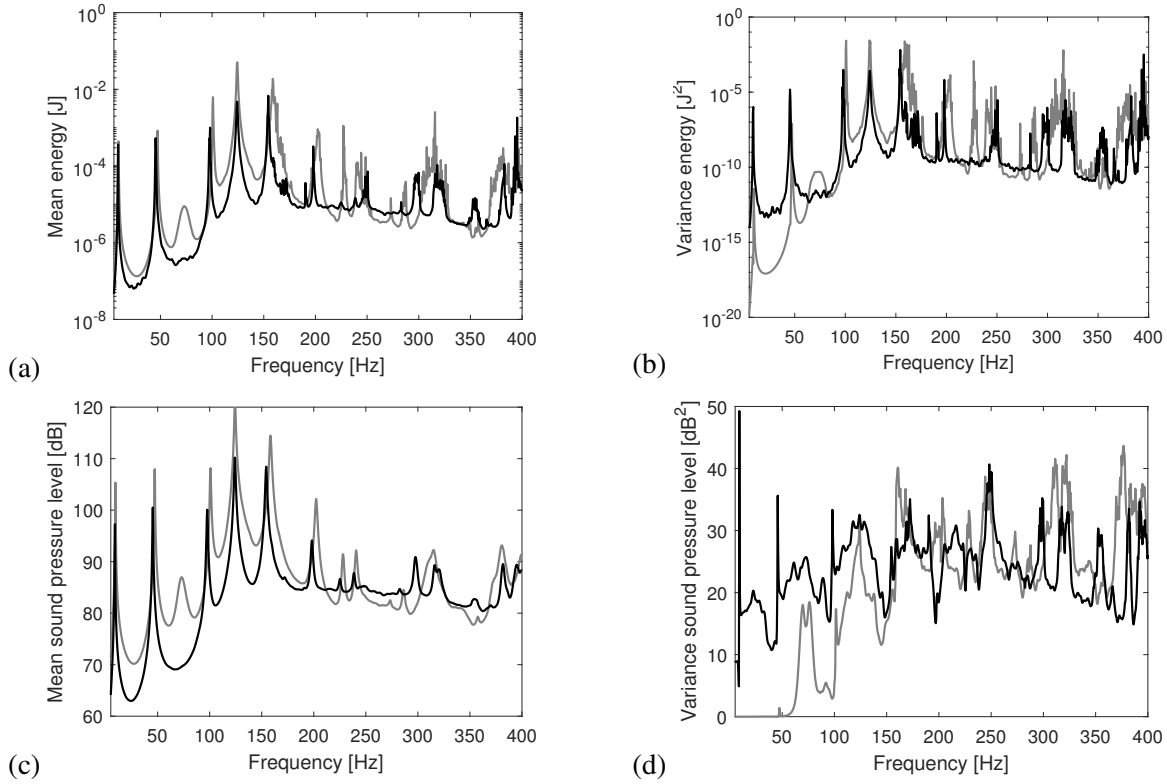

Figure 4. Ensemble average (left: (a) and (c)) and variance (right:(b) and (d)) of the total energy (top: (a) and (b)) and sound pressure level (bottom: (c) and (d)) in the acoustic cavity. The results of the detailed MC approach are indicated with grey lines, the results of the GOE-MC approach with black lines.

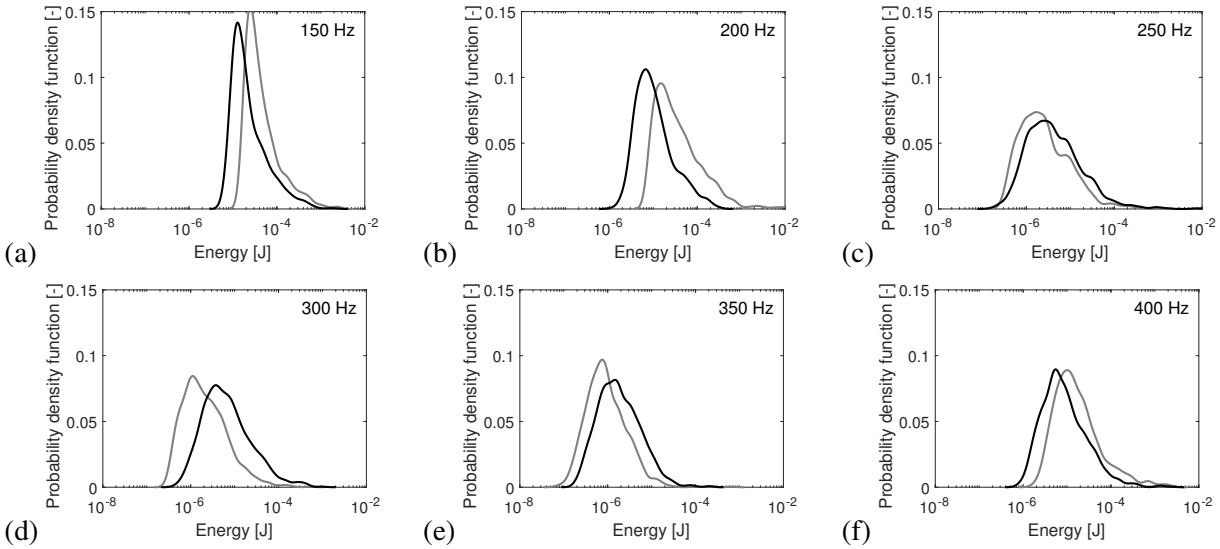

Figure 5. Probability density function of the total energy in the acoustic cavity at 6 frequencies. The results of the detailed MC approach are indicated with grey lines, the results of the GOE-MC approach with black lines.

nents. The response of these systems has been obtained by generating these coupling term realizations. The presented approach is validated for the problem of sound radiation into an aircraft cabin. It is illustrated that the diffuse field modelling approach is able to correctly predict the probability distribution of energetic quantities, except at very low frequencies, where the small random wave scatterers have a minor influence on the local sound field, and the diffuse field model overestimates the related uncertainty.

7. ACKNOWLEDGEMENTS

This research was funded by the European Research Council (ERC), in the form of the ERC Starting Grant 714591 VirBAcous. The financial support is gratefully acknowledged.

8. REFERENCES

[1] R. Langley and J. Cordioli, "Hybrid deterministic-statistic analysis of vibro-acoustic systems with domain couplings on statistical components," *Journal of Sound and Vibration*, vol. 321, no. 3–5, pp. 893–912, 2009.

[2] E. Reynders, J. Legault, and R. Langley, "An efficient probabilistic approach to vibro-acoustic analysis based on the Gaussian orthogonal ensemble," *Journal of the Acoustical Society of America*, vol. 136, no. 1, pp. 201–212, 2014.

[3] C. Van hoorickx and E. Reynders, "Gaussian orthogonal ensemble modeling of built-up systems containing general diffuse components and parametric uncertainty," *Journal of Sound and Vibration*, vol. 501, no. 116045, pp. 1–18, 2021. Open access.

[4] C. Van hoorickx and E. Reynders, "Numerical realization of diffuse sound pressure fields using prolate spheroidal wave functions," *Journal of the Acoustical Society of America*, vol. 151, no. 3, pp. 1710–1721, 2022. Open access.

[5] E. Wigner, "On the distribution of the roots of certain symmetric matrices," *Annals of Mathematics*, vol. 67, no. 2, pp. 325–327, 1958.

[6] R. Weaver and O. Lobkis, "Diffuse fields in open systems and the emergence of the Green's function (L)," *Journal of the Acoustical Society of America*, vol. 116, no. 5, pp. 2731–2734, 2004.

[7] M. V. Berry, "Regular and irregular semiclassical wavefunctions," *Journal of Physics A: Mathematical and Theoretical*, vol. 10, no. 12, pp. 2083–2091, 1977.

[8] B. Van Genechten, D. Vandepitte, and W. Desmet, "A direct hybrid finite element – Wave based modelling technique for efficient coupled vibro-acoustic analysis," *Computer Methods in Applied Mechanics and Engineering*, vol. 200, no. 5–8, pp. 742–764, 2011.

[9] M. Niu, *Airframe Structural Design*. Hong Kong: Conmilit Press, 1988.

[10] K. Bathe, *Finite Element Procedures*. Englewood Cliffs, NJ: Prentice-Hall, second ed., 1996.

[11] O. Zienkiewicz and R. Taylor, *The finite element method, Volume 1: the basis*. Oxford, United Kingdom: Butterworth-Heinemann, fifth ed., 2000.

[12] O. Zienkiewicz and R. Taylor, *The finite element method, Volume 2: solid mechanics*. Oxford, United Kingdom: Butterworth-Heinemann, fifth ed., 2000.

[13] L. Meirovitch, *Elements of vibration analysis*. New York, NY: McGraw-Hill, 2nd ed., 1986.

[14] R. Craig and A. Kurdila, *Fundamentals of structural dynamics*. Hoboken, NJ: John Wiley & Sons, 2nd ed., 2006.

[15] R. Langley and V. Cotoni, "Response variance prediction in the statistical energy analysis of built-up systems," *Journal of the Acoustical Society of America*, vol. 115, no. 2, pp. 706–718, 2004.

[16] R. Langley and V. Cotoni, "Response variance prediction for uncertain vibro-acoustic systems using a hybrid deterministic-statistical method," *Journal of the Acoustical Society of America*, vol. 122, no. 6, pp. 3445–3463, 2007.

[17] A. Cicirello and R. Langley, "The vibro-acoustic analysis of built-up systems using a hybrid method with parametric and non-parametric uncertainties," *Journal of Sound and Vibration*, vol. 332, no. 9, pp. 2165–2178, 2013.

[18] R. Lyon and R. DeJong, *Theory and application of statistical energy analysis*. Newton, MA: Butterworth-Heinemann, second ed., 1995.

[19] A. Pierce, *Acoustics: an introduction to its physical principles and applications*. Cham, Switzerland: Springer, 3rd ed., 2019.